Regional histopathology and prostate MRI positivity: a secondary analysis of the PROMIS trial

Journal:	*Radiology*
Manuscript ID	RAD-22-0762.R3
Manuscript Type:	Original Research
Manuscript Categorization Terms:	Adults < 1. SUBJECT MATTER, MR-Imaging < 3. MODALITIES/TECHNIQUES, Biopsy/Needle Aspiration < 4. PROCEDURES, Urinary < 5. AREAS/SYSTEMS, Prostate < 6. STRUCTURES, Neoplasms-Primary < 7. TOPICS

Regional histopathology and prostate MRI positivity: a secondary analysis of the PROMIS trial

Vasilis Stavrinides[1,2,3], Joseph M. Norris[1,3], Solon Karapanagiotis[2,4], Francesco Giganti[1,5], Alistair Grey[1,3], Nick Trahearn[6], Alex Freeman[7], Aiman Haider[7], Lina Maria Carmona Echeverria[1,7], Simon R.J. Bott[8], Louise C. Brown[9], Nicholas Burns-Cox[10], Timothy J. Dudderidge[11], Ahmed El-Shater Bosaily[12], Maneesh Ghei[13], Alastair Henderson[14], Richard G. Hindley[15], Richard S. Kaplan[9], Robert Oldroyd[16], Chris Parker[17], Raj Persad[18], Derek J. Rosario[19], Iqbal S. Shergill[20], Mathias Winkler[21,22], Alex Kirkham[5], Shonit Punwani[1,5,23], Hayley C. Whitaker[1], Hashim U. Ahmed*[21,22], Mark Emberton*[1,3], on behalf of the PROMIS group

* Joint senior authors

[1] UCL Division of Surgery & Interventional Science, University College London, London, UK

[2] The Alan Turing Institute, London, UK

[3] Department of Urology, University College London Hospitals NHS Foundation Trust, London, UK

[4] Medical Research Council (MRC) Biostatistics Unit, University of Cambridge, Cambridge, UK

[5] Department of Radiology, University College London Hospitals NHS Foundation Trust, London, UK

[6] Computational Pathology Group, Institute of Cancer Research, Sutton, London, UK

[7] Department of Pathology, University College London Hospitals NHS Foundation Trust, London, UK

[8] Department of Urology, Frimley Health NHS Foundation Trust, London, UK

[9] Medical Research Council (MRC) Clinical Trials Unit, University College London, London, UK

[10] Department of Urology, Taunton & Somerset NHS Foundation Trust, Taunton, UK

[11] Department of Urology, University Hospital Southampton NHS Foundation Trust, Southampton, UK

[12] Department of Radiology, Royal Free London NHS Foundation Trust, London, UK

[13] Department of Urology, Whittington Health NHS Trust, London, UK

[14] Department of Urology, Maidstone & Tunbridge Wells NHS Trust, Tunbridge Wells, UK
[15] Department of Urology, Hampshire Hospitals NHS Foundation Trust, UK
[16] Public and patient representative, Nottingham, UK
[17] Department of Academic Urology, The Royal Marsden NHS Foundation Trust, Sutton, UK
[18] Department of Urology, North Bristol NHS Trust, Bristol, UK
[19] Department of Urology, Sheffield Teaching Hospitals NHS Foundation Trust, Sheffield, UK
[20] Department of Urology, Wrexham Maelor Hospital NHS Trust, Wrexham, UK
[21] Department of Urology, Imperial College Healthcare NHS Trust, London, UK
[22] Imperial Prostate, Division of Surgery, Department of Surgery & Cancer, Faculty of Medicine, Imperial College London, London, UK
[23] Centre for Medical Imaging, University College London, London, UK

Corresponding author:

Vasilis Stavrinides

Division of Surgery and Interventional Science, University College London

Charles Bell House, 43-45 Foley Street, London W1W 7TS, United Kingdom

v.stavrinides@ucl.ac.uk

Keywords: Barzell zone, MRI, PROMIS, prostate cancer.

Ethics: Ethical approval for PROMIS was granted by the National Research Ethics Service Committee London (Ref: 11/LO/0185).

Funding and acknowledgements: This manuscript and the data used in the analysis was provided from the PROMIS study. PROMIS was funded by the UK Government Department of Health, National Institute of Health Research–Health Technology Assessment Programme, (Project number 09/22/67). Support was also provided by National Institute for Health

Research (NIHR) UCLH/UCL Biomedical Research Centre, National Institute for Health Research (NIHR) The Royal Marsden and Institute for Cancer Research Biomedical Research Centre and National Institute for Health Research (NIHR) Imperial Biomedical Research Centre. The original PROMIS study was coordinated by the Medical Research Council Clinical Trials Unit (MRC CTU) at UCL and sponsored by University College London (UCL). The PROMIS Biobank was funded by Prostate Cancer UK (PG10-17). The PROMIS dataset and the biobank is under the research governance of the ReIMAGINE Risk Trial Management Group funded by Medical Research Council (UKRI; MR/R014043/1) and Cancer Research UK.

The analysis presented here was further funded by the UK Medical Research Council (UKRI) through a Clinical Research Training Fellowship awarded to VS (MR/S005897/1); data was obtained by the ReIMAGINE Consortium (reference PB0001D). VS acknowledges funding from the European Association of Cancer Research (EACR Travel Fellowship), the Mason Medical Research Foundation, Prostate Cancer UK (UCL-UCLH Centre of Excellence Fund), Cancer Research UK (EDDAMC-2021\100001) and the Alan Turing Institute (EPSRC grant EP/N510129/1).

Conflicts of interest: HA research is supported by core funding from the United Kingdom's National Institute of Health Research (NIHR) Imperial Biomedical Research Centre. He currently receives funding from the Wellcome Trust, Medical Research Council (UK), Cancer Research UK, Prostate Cancer UK, National Institute for Health Research (UK), The Urology Foundation, BMA Foundation, Imperial Health Charity, NIHR Imperial BRC, Sonacare Inc,

Trod Medical and Sophiris Biocorp for trials in prostate cancer. He was a paid medical consultant for Sophiris Biocorp in the previous 3 years. He is a proctor for HIFU and cryotherapy and paid for training other surgeons in this procedure. ME serves as a consultant/educator/trainer for Sonacare, Exact Imaging, Angiodynamics, and Profound Medical; and receives research support from the NIHR UCLH/UCL Biomedical Research Centre. Freeman and Kirkham have shares in Nuada Medical Ltd. Hindley has stock or share interest with Nuada and is Clinical Director for the Prostate Care Division and has also received funding from Sonacare for teaching and training. Norris receives research funding from the MRC. Punwani has sessional funding from UCLH BRC. The other authors declare no competing interests.

Regional histopathology and prostate MRI positivity: a secondary analysis of the PROMIS trial

Key Results:

- In 161 men from the PROMIS trial, prostate zones that contained Gleason 3+4 cancer were three times more likely to be MRI-positive than benign zones (OR: 3.1 p<0.001), and almost nine times if they contained Gleason ≥4+3 (OR: 8.7, p<0.001).
- Increasing maximum cancer core length raised the odds of a cancerous zone being MRI-positive (OR: 1.24 per mm increase, p<0.001).
- In cancer-free prostates, zones containing prostatic intraepithelial neoplasia were more likely to be MRI-positive (OR: 3.7, p=0.004).

Summary: There is a incremental relationship between prostate cancer burden and the likelihood of a positive MRI signal.

Abbreviations:

csCa: Clinically Significant Cancer

ISUP: International Society of Urological Pathology

MCCL: Maximum Cancer Core Length

OR: Odds Ratio

PSA: Prostate-Specific Antigen

PIN: Prostatic Intraepithelial Neoplasia

PROMIS: Prostate MRI Imaging Study

TPM: Transperineal Mapping

UCL: University College London

10 E. Doty St., Suite 441, Madison, WI 53703, 630-481-1047, radiology@rsna.org

Abstract

Background: The effects of regional histopathological changes on prostate MRI have not been accurately quantified in men with elevated PSA and no previous biopsy.

Purpose: To assess how Gleason grade, maximum cancer core length (MCCL), inflammation, prostatic intraepithelial neoplasia (PIN) or atypical small acinar proliferation within a Barzell zone affects its odds of being MRI-visible.

Materials and Methods: In this secondary analysis of the PROMIS trial (NCT01292291; May 2012 to November 2015), consecutive participants who underwent mpMRI followed by a combined biopsy, including 5-mm trans perineal mapping (TPM), were evaluated. TPM pathology was reported at the whole-prostate level and for each of 20 Barzell zones per prostate. An expert panel blinded to pathology reviewed MRIs and declared which Barzell areas spanned Likert 3-5 lesions. The relationship of Gleason grade and MCCL to zonal MRI outcome ("visible", "non-visible") was assessed using generalized linear mixed effects models with random intercepts for individual patients. Inflammation, PIN and atypical small acinar proliferation were similarly assessed in trans-perineal mapping-negative men.

Results: The panel evaluated 161 men (median age, 62y [IQR, 11]) and assigned MRI status to 3179 Barzell zones. Compared to benign areas, the odds of MRI-visibility were higher when a zone contained Gleason 3+4 (odds ratio [OR] 3.1; 95%CI: 1.9-4.9, $p<0.001$) or Gleason ≥4+3 cancer (OR 8.7; 95%CI: 4.5-17.0, $p<0.001$). MCCL also determined visibility (OR 1.24 per mm increase; 95%CI: 1.15-1.33, $p<0.001$) but odds were lower with each

10 E. Doty St., Suite 441, Madison, WI 53703, 630-481-1047, radiology@rsna.org

prostate volume doubling (OR 0.7; 95%CI: 0.5-0.9). In trans perineal mapping-negative men, PIN increased the odds of zonal visibility (OR 3.7; 95%CI: 1.5-9.1, p=0.004).

Conclusion: There is an incremental relationship between cancer burden and prostate MRI visibility. Prostatic intraepithelial neoplasia contributed to false positive MRI.

10 E. Doty St., Suite 441, Madison, WI 53703, 630-481-1047, radiology@rsna.org

1. Introduction

MRI signal in the human prostate is generated by biological processes with microstructural implications. For example, MRI-visible, clinically significant cancer (csCa) is associated with increased cellularity and decreased luminal density; whereas, false positives are considered a by-product of non-malignant microenvironmental perturbations, such as inflammation.[1–3] In men without prior biopsy and raised prostate-specific antigen (PSA), a quantitative understanding of the relationship between regional pathology and MRI positivity is a pre-requisite for distinguishing true from false positives and mitigating unnecessary MRI-directed sampling.[4] Unfortunately, as it is particularly difficult to comprehensively capture all possible MRI phenotypes in unperturbed prostates, many studies are afflicted by selection, spectrum, or sampling bias.

We recently studied a well-interrogated, biopsy-naïve population from the PROMIS trial to lay out a clinically useful distinction between true and false positive MRI through the use of readily available radiological scores, PSA density, lesion volume and diffusion restriction metrics.[5,6] In brief, PROMIS was a multicentre, paired cohort study that investigated the diagnostic accuracy of multiparametric MRI versus systematic transrectal ultrasound-guided (TRUS) biopsy against a reference standard (transperineal prostate mapping, or TPM, a highly accurate sampling technique where the prostate is sampled every 5 mm). The study proved that, in men with raised PSA and suspected cancer, mpMRI detects more clinically significant disease with fewer needle deployments, whereas TRUS biopsies miss up to half

10 E. Doty St., Suite 441, Madison, WI 53703, 630-481-1047, radiology@rsna.org

of significant tumours. At the same time, mpMRI picks up 5% fewer insignificant cancers compared to TRUS-guided sampling. The fact that the study was blinded (i.e. MRI interpretation and combined TPM-TRUS biopsy were independent) and that such a rigorous reference standard was applied in previously biopsy-naïve men gives PROMIS its unique advantage, which is its relative freedom from spectrum, selection and sampling biases. Due to the study's uniqueness, it would be perhaps helpful for the reader to review its original design (see also Supplementary Figure 1).[5]

The purpose of the work presented here was to assess how Gleason grade, maximum cancer core length (MCCL), inflammation, prostatic intraepithelial neoplasia (PIN) or atypical small acinar proliferation within a Barzell zone affects its odds of being MRI-visible. In the process, we propose a Barzell zone-based framework of MRI positivity and demonstrate a simple method for aligning biopsy findings to MRI that, despite its coarseness, could be useful in settings where computer-based MRI-histology registration is impossible.

10 E. Doty St., Suite 441, Madison, WI 53703, 630-481-1047, radiology@rsna.org

2. Materials and methods

2.1. Participants and Data

In total, 576 biopsy-naïve men with elevated PSA (≤ 15ng/mL) were recruited in the original multicenter PROMIS study (ClinicalTrials.gov: NCT01292291) between May 2012 and November 2015.[5] Ethics committee approval for PROMIS was originally granted by National Research Ethics Service Committee London (reference 11/LO/0185) and all patients provided written informed consent. Data analyzed for this study were provided by a third party. Requests for data should be directed to the provider indicated in the Acknowledgments. Briefly, all men underwent pre-biopsy 1.5 Tesla multiparametric MRI (mpMRI) followed by a combined biopsy procedure under general anaesthetic (5-mm TPM followed by standard systematic transrectal biopsy) performed by clinicians blinded to imaging findings. Standard reporting within PROMIS included age, presenting PSA, as well as per-patient, overall TPM pathology designated by a uro-pathologist after considering global prostate cancer burden through Gleason score and maximum cancer core length (MCCL) according to International Society of Urological Pathology (ISUP) and UK standards.[7] Overall TPM pathology was used in PROMIS as the “ground truth” and resulted in classification of all prostates according to four well-established University College London definitions: 1) no cancer; 2) insignificant cancer (Gleason 3+3 with MCCL up to 4 mm); 3) definition 2 csCa (any Gleason ≥3+4 and/or any grade MCCL ≥4 mm); and 4) definition 1 csCa (any Gleason score ≥4+3 and/or any grade MCCL ≥6 mm).

10 E. Doty St., Suite 441, Madison, WI 53703, 630-481-1047, radiology@rsna.org

In a previous article, we considered a subgroup of consecutive PROMIS participants recruited only at University College London.[6] This prior work dealt with clinical-radiological characteristics (e.g. PSA density, apparent diffusion coefficient [ADC]) that distinguish MRI true and false positives, using prostate-level TPM results as a reference standard. In this manuscript we quantify the direct impact of regional prostate pathology on MRI visibility since, for consecutive PROMIS non-pilots, TPM pathology was also reported per Barzell zone. The 20-zone modified Barzell scheme has been described previously and has been used in University College London trials (Supplementary Figure 1).[8] Per-zone reporting included Gleason and MCCL information whenever cancer was detected; whereas in non-cancerous zones, the presence of inflammation, PIN and atypical small acinar proliferation was reported in a binary fashion (present or non-present). From a radiological standpoint, apart from prostate volume (calculated on MRI using the ellipsoid formula) and overall, per-prostate Likert scores for underlying csCa, information was additionally recorded at the lesion level (including per-sequence Likert scores, location, volume, and Apparent Diffusion Coefficient [ADC]).

2.2. Consensus Alignment of Modified Barzell Zones to mpMRI lesions (Likert ≥ 3)

Completely anonymised MRI images were retrieved and randomly reviewed by a multidisciplinary panel consisting of a uro-radiologist (FG; 8 years of experience in prostate MRI reporting), a urologist (AG; 10 years of experience in prostate intervention and MRI

10 E. Doty St., Suite 441, Madison, WI 53703, 630-481-1047, radiology@rsna.org

interpretation) and two uro-pathologists (AF, AH; 20 and 6 years of experience in uro-pathology) blinded to TPM findings. After assessing each MRI separately (T2, ADC map, long-b and dynamic contrast-enhanced sequences) and using a Barzell zone map as a guide, the panel was asked to declare by consensus which zones were “MRI-visible” (i.e. spanned by a Likert ≥ 3 lesion) and which were “non-visible”. If an MRI lesion covered more than one Barzell zone, the panel was also asked to declare which zone “aligned best” with the lesion and designate its “non-visible” counterpart in the most appropriate distant area (mirror position whenever possible).[9] After these steps and once the panel had finished assigning an MRI outcome to all zones, TPM pathology was revealed: lesions spanning at least one “MRI-visible”, csCa-containing zone (according to University College London definitions) were deemed “true positives”, whereas lesions that did not span any such zones were considered “false positives”.

2.3. Statistical Analysis

Continuous and categorical characteristics were summarized using simple statistics such as means, medians, interquartile ranges (IQRs) and proportions. Non-parametric tests (Wilcoxon, Kruskal-Wallis analysis of variance) were used to detect between-group differences. To investigate the relationship between Barzell zone pathology and the odds of that same zone being declared MRI visible by the expert panel, we used mixed effects logistic regression models with a binary outcome (visible or non-visible zone) and pathological variables as predictors (e.g. Gleason, MCCL etc). Since there were 20 Barzell zones per

10 E. Doty St., Suite 441, Madison, WI 53703, 630-481-1047, radiology@rsna.org

participant, we included random intercepts for individual patients to account for within-patient correlation and scrutinised this approach against a generalised linear model with fixed predictors only. The final model selection was based on the Akaike Information Criterion. The R statistical software (version 4.1.2, R Foundation for Statistical Computing; http://www.R-project.org/) was used for all analyses, and all p-values were considered significant at the .05 level.

3. Results

3.1. Patient Characteristics Stratified by Per-Prostate Gleason Grade

Among the 576 men in the PROMIS trial, a subset of patients from a single institution, University College London, were considered. Of those, 161 non-pilot patients met the criteria for this secondary analysis (median age, 62 [IQR, 11] years), while 78 pilot patients were excluded (Figure 1A). Age, presenting PSA, PSA density and prostate volume are shown in Table 1 for all men and stratified by overall Gleason on TPM which, as described, was designated by the study uro-pathologist. Although the four Gleason groups were not substantially different in terms of age at first biopsy, pairwise comparisons revealed an important association of PSA density and prostate volume with grade (Figures 2A, 2B and 2C). The largest differences in PSA density and volume were observed between men with Gleason ≥4+3 cancer and no cancer on TPM ($p<.001$, Wilcoxon test), while men with 3+4 and 3+3 disease fell between those two extremes.

3.2. Zonal Gleason and Maximum Cancer Core Length as Predictors of MRI Positivity (all men)

The workflow followed by the panel is presented in Figure 1A. Of 3179 zones reviewed, 2516 (79.1%) were benign, 301 (9.5%) had Gleason 3+3 cancer, 271 (8.5%) had Gleason 3+4, and 91 (2.9%) zones had Gleason ≥ 4+3 (4+3: 73, 4+4: 11, 4+5: 6 and 3+5: 1). The panel

10 E. Doty St., Suite 441, Madison, WI 53703, 630-481-1047, radiology@rsna.org

concluded that 595 of 3179 zones in total were MRI-positive (18.7%), and this proportion clearly depended on cancer burden (Figure 1B): 319 of 2516 (12.7%) benign zones, 69 of 301 (22.9%) Gleason 3+3 zones, 144 of 271 (53.1%) Gleason 3+4 zones, and 63 of 91 (69%) Gleason ≥ 4+3 zones (4+3: 49/73; 4+4: 7/11; 4+5: 6/6; 3+5: 1/1) were MRI-positive. The proportion of MRI-positive cancerous zones increased with MCCL regardless of Gleason grade (Figure 1B).

Based on these observations, mixed effects logistic regression models with random intercepts for individual patients and zonal MRI positivity as a binary outcome (visible, non-visible) were fitted to the data. The final mixed model included zonal Gleason grade, ISUP MCCL in mm, and the $\log_2$ of prostate volume (in mL) as predictors and performed better than intercept-only baseline models or models with each predictor alone (Table 2, Supplementary Table 1). Gleason grades 3+4 and ≥4+3 were both significantly associated with outcome ($p<0.001$), increasing the likelihood of a zone being “MRI-positive” three-fold (odds ratio [OR]: 3.1; 95%CI: 1.9-4.9, $p<0.001$) and almost nine-fold (OR: 8.7; 95%CI: 4.5-16.6, $p<0.001$), respectively. MCCL was also a predictor of zonal MRI positivity, with each additional mm corresponding to an OR of 1.24 (95% CI: 1.15-1.33, $p<0.001$) regardless of Gleason grade. Finally, in line with our initial observations on prostate volume, every volume doubling was associated with reduced odds of zonal MRI positivity (OR: 0.7; 95%CI: 0.5-0.9, $p=0.02$). The model-predicted probabilities of zonal MRI positivity are presented in Figure 3B for different combinations of Gleason, MCCL and prostate volume.

3.3. Zonal Inflammation, PIN and atypical small acinar proliferation as predictors of false MRI positivity (TPM-negative men)

Mixed effects logistic regression models were fitted with random intercepts for patients who were TPM-negative (n=52). In these models panel-designated zonal MRI visibility was again a binary outcome, whereas inflammation, PIN or atypical small acinar proliferation status within the zone was represented as the linear combination of three binary predictors (present, non-present). In an initial model including all three binary variables (Table 3), only PIN predicted zonal MRI positivity (OR: 3.2; 95%CI: 1.3-8.1, p=0.01). After successive model fitting a final, reduced mixed model indicated that, in TPM-negative prostates, the presence of PIN in a Barzell zone almost quadrupled its odds of being MRI-visible (OR: 3.3; 95%CI: 1.5-9.1, p=0.004; Table 3 and Supplementary Table 1).

4. Discussion

In this study, we quantified the impact of prostatic pathology on regional MRI visibility in men undergoing their first PSA-triggered biopsy. We found the presence of a Gleason 4 component substantially increases the odds of Barzell zone being MRI-positive compared to benign tissue (OR 3.1 for Gleason 3+4), particularly when more aggressive patterns are dominant (OR 8.7 for Gleason ≥4+3). Maximum cancer core length (MCCL) increments had an additive effect on the odds of zonal MRI positivity regardless of Gleason (OR 1.24 per mm increase), re-iterating the need to consider more than grade when addressing MRI-related questions in the prostate. For example, University College London definitions allow MCCL to be a dominant feature of clinical significance in patients with low Gleason and, in our model, Gleason 3+3 could theoretically elicit zonal MRI positivity provided MCCL is high enough.[10] The usefulness of such schemes is corroborated by the fact that University College London definitions were also highly predictive of zonal MRI visibility in mixed models (Supplementary Figure A). When assessing MRI scores of cancerous Barzell zones, we confirmed that high Gleason and MCCL are particularly associated with Likert of 4 and 5, in contrast to insignificant disease that elicits mainly indeterminate phenotypes (Supplementary Figure B). These conclusions are complementary to previously published work confirming false negativity is mostly associated with lower grade and small MCCL.[11]

The link we found between PIN and MRI false positives has been described by others.[12] However, PIN is spatially proximal to prostate cancer and, although TPM is the best possible

reference standard in a biopsy-naïve population, there is an unavoidable 5-10% chance of misclassification that could positively bias associations between PIN and false positive MRI.[10,13,14] Interestingly, our findings on inflammation do not fit the dominant narrative regarding cancer-negative lesions, almost half of which reportedly contain inflammatory foci.[15–17] However, we would not immediately interpret our results as evidence against inflammation driving MRI false positives as PROMIS did not have MRI-directed sampling, which appears to capture microenvironmental perturbations better than non-targeted needle deployments.[18] We also suspect that, although the spatial conformation of immune cells is as important as their count in terms of tissue microstructure, pathologists report inflammation based mostly on the latter.

Finally, we found two “extreme” prostate states captured by TPM: one involving small organs with high csCa burden and the other involving prostates without csCa, where PSA is mainly driven by high organ volume. These extremes and conditions in-between were not age-related. We previously calculated that the MRI volume of prostates with actively surveyed insignificant disease increases by ~3.3 mL/year, starting, on average, at about 50 mL at MRI diagnosis (at around 63 years).[19,20] This starting point is close to the median age and volume of csCa-free men in this study, but is not compatible with the median prostate volume of men with overall Gleason ≥4+3 on TPM (which stood at 39 mL despite a slightly greater median age at 64 years). Altogether, these observations raise the question of whether there are two distinct pathologies intercepted by the first PSA-triggered, MRI-informed biopsy, which would lead to two clinical scenarios: one associated with the early detection of csCa in small

prostates not undergoing significant age-related growth, and a second where sampling of already enlarged prostates identifies, on occasion, insignificant disease that either remains stable or progresses over several years while prostatic enlargement continues regardless.

Our study had limitations. First, the inherent coarseness of consensus-based TPM-MRI alignment would explain the herein unexplored but inevitable discrepancies between the prostate-level analyses of PROMIS and our more involved, zone-level examination. This is a direct consequence of PROMIS lacking MRI-directed sampling, which was a necessary compromise for keeping the study investigators blind to pathology and imaging. Second, TPM without targeting almost certainly underestimates Gleason pattern 4 and MCCL: deploying a needle towards the lesion centre leads to correct grade attribution in 80% of heterogenous tumours, but a direct hit in the orientation with the greatest yield is less likely with 5 mm TPM sampling.[21] Head-to-head comparisons of MRI targeting and TPM in treatment-naïve men and those with radio-recurrence confirm that, although both biopsy approaches have good detection rates for csCa, MRI targeting captures slightly more high-grade cancers with less needle deployments whereas TPM detects more small, low-grade lesions.[22,23] Third, one could rightly argue that MRI acquisition and interpretation changed since PROMIS, which is one of the reasons we do not claim our findings are immediately generalizable. However, we suspect our consensus alignment approach could be useful and applicable in other MRI-informed biopsy settings.

In conclusion, the results of this study provide a basis for the MRI signals observed in the prostate. There is an incremental relationship between cancer burden and prostate MRI visibility. Prostatic intraepithelial neoplasia contributes to false positive MRI. Future work will involve a systematic digital histopathological evaluation of specific microstructural features associated with different MRI endotypes and how the interaction between different pathological entities (e.g. cancer and inflammation) affects MRI characteristics.

References

1. Chatterjee, A. *et al.* Changes in Epithelium, Stroma, and Lumen Space Correlate More Strongly with Gleason Pattern and Are Stronger Predictors of Prostate ADC Changes than Cellularity Metrics. *Radiology* **277**, 751–762 (2015).
2. Miyai, K. *et al.* Histological differences in cancer cells, stroma, and luminal spaces strongly correlate with in vivo MRI-detectability of prostate cancer. *Mod. Pathol.* **32**, 1536–1543 (2019).
3. Panebianco, V. *et al.* An update of pitfalls in prostate mpMRI: a practical approach through the lens of PI-RADS v. 2 guidelines. *Insights Imaging* **9**, 87–101 (2018).
4. Bangma, C. H., van Leenders, G. J. L. H., Roobol, M. J. & Schoots, I. G. Restricting False-positive Magnetic Resonance Imaging Scans to Reduce Overdiagnosis of Prostate Cancer. *Eur. Urol.* (2020). doi:10.1016/j.eururo.2020.10.013
5. Ahmed, H. U. *et al.* Diagnostic accuracy of multi-parametric MRI and TRUS biopsy in prostate cancer (PROMIS): a paired validating confirmatory study. *The Lancet* **389**, 815–822 (2017).
6. Stavrinides, V. *et al.* False Positive Multiparametric Magnetic Resonance Imaging Phenotypes in the Biopsy-naïve Prostate: Are They Distinct from Significant Cancer-associated Lesions? Lessons from PROMIS. *Eur. Urol.* S0302283820307703 (2020). doi:10.1016/j.eururo.2020.09.043
7. van Leenders, G. J. L. H. *et al.* The 2019 International Society of Urological Pathology (ISUP) Consensus Conference on Grading of Prostatic Carcinoma. *Am. J. Surg. Pathol.* **44**, e87–e99 (2020).
8. Simmons, L. A. M. *et al.* The PICTURE study: diagnostic accuracy of multiparametric MRI in men requiring a repeat prostate biopsy. *Br. J. Cancer* **116**, 1159–1165 (2017).

9. Giganti, F. *et al.* DWI and PRECISE criteria in men on active surveillance for prostate cancer: A multicentre preliminary experience of different ADC calculations. *Magn. Reson. Imaging* **67**, 50–58 (2020).
10. Ahmed, H. U. *et al.* Characterizing Clinically Significant Prostate Cancer Using Template Prostate Mapping Biopsy. *J. Urol.* **186**, 458–464 (2011).
11. Norris, J. M. *et al.* What Type of Prostate Cancer Is Systematically Overlooked by Multiparametric Magnetic Resonance Imaging? An Analysis from the PROMIS Cohort. *Eur. Urol.* **78**, 163–170 (2020).
12. Tosoian, J. J., Alam, R., Ball, M. W., Carter, H. B. & Epstein, J. I. Managing high-grade prostatic intraepithelial neoplasia (HGPIN) and atypical glands on prostate biopsy. *Nat. Rev. Urol.* **15**, 55–66 (2018).
13. Hu, Y. *et al.* A biopsy simulation study to assess the accuracy of several transrectal ultrasonography (TRUS)-biopsy strategies compared with template prostate mapping biopsies in patients who have undergone radical prostatectomy: REPEAT TRUS-GUIDED BIOPSY vs TEMPLATE PROSTATE MAPPING. *BJU Int.* **110**, 812–820 (2012).
14. Sakr, W. A. *et al.* High grade prostatic intraepithelial neoplasia (HGPIN) and prostatic adenocarcinoma between the ages of 20-69: an autopsy study of 249 cases. *Vivo Athens Greece* **8**, 439–443 (1994).
15. Jyoti, R., Jina, N. H. & Haxhimolla, H. Z. In-gantry MRI guided prostate biopsy diagnosis of prostatitis and its relationship with PIRADS V.2 based score. *J. Med. Imaging Radiat. Oncol.* **61**, 212–215 (2017).
16. Gordetsky, J. B. *et al.* Histologic findings associated with false-positive multiparametric magnetic resonance imaging performed for prostate cancer detection. *Hum. Pathol.* **83**, 159–165 (2019).

17. Rourke, E. *et al.* Inflammation appears as high Prostate Imaging–Reporting and Data System scores on prostate magnetic resonance imaging (MRI) leading to false positive MRI fusion biopsy. *Investig. Clin. Urol.* **60**, 388 (2019).
18. Hupe, M. C. *et al.* Histomorphological analysis of false positive PI-RADS 4 and 5 lesions. *Urol. Oncol. Semin. Orig. Investig.* (2020). doi:10.1016/j.urolonc.2020.01.017
19. Stavrinides, V. *et al.* Five-year Outcomes of Magnetic Resonance Imaging–based Active Surveillance for Prostate Cancer: A Large Cohort Study. *Eur. Urol.* (2020). doi:10.1016/j.eururo.2020.03.035
20. Stavrinides, V. *et al.* Mapping PSA density to outcome of MRI-based active surveillance for prostate cancer through joint longitudinal-survival models. *Prostate Cancer Prostatic Dis.* **24**, 1028–1031 (2021).
21. El-Shater Bosaily, A. *et al.* The concordance between the volume hotspot and the grade hotspot: a 3-D reconstructive model using the pathology outputs from the PROMIS trial. *Prostate Cancer Prostatic Dis.* **19**, 258–263 (2016).
22. Kanthabalan, A. *et al.* Transperineal Magnetic Resonance Imaging-targeted Biopsy versus Transperineal Template Prostate Mapping Biopsy in the Detection of Localised Radio-recurrent Prostate Cancer. *Clin. Oncol.* **28**, 568–576 (2016).
23. Kaufmann, B. *et al.* Prostate cancer detection rate in men undergoing transperineal template-guided saturation and targeted prostate biopsy. *The Prostate* **82**, 388–396 (2022).

10 E. Doty St., Suite 441, Madison, WI 53703, 630-481-1047, radiology@rsna.org

Tables

Table 1: Baseline Characteristics of Included UCLH Non-Pilot Patients (n=161)

Overall Gleason on TPM	Benign	Gleason 3+3	Gleason 3+4	Gleason 4+3	All patients
n (%)	52 (33%)	21 (13%)	60 (37%)	28 (17%)	161
Age (y)	62 (9)	59 (12)	63.5 (10.2)	64 (14.2)	62 (11)
Prostate volume (mL)	55.5 (18.8)	45 (23)	40 (24)	39 (16.2)	44 (25)
PSA (ng/mL)	4.85 (2.25)	4.8 (2.4)	6.15 (3)	9.35 (2.5)	6 (3.6)
PSAD (ng/mL^2)	0.09 (0.05)	0.10 (0.06)	0.16 (0.12)	0.25 (0.14)	0.13 (0.12)

Note.--Age, prostate volume, prostate specific antigen (PSA) and PSA density (PSAD) are presented for the entire cohort and for each overall Gleason group as assigned by the study uro-pathologists. Unless otherwise noted, data presented as median with IQR given in parentheses. TPM = trans-perineal mapping, UCLH = University College London Hospital.

10 E. Doty St., Suite 441, Madison, WI 53703, 630-481-1047, radiology@rsna.org

Table 2: Mixed Model of Cancer Burden and Prostate Volume as Predictors of Zonal MRI Visibility in Non-Pilot Patients (n=161)

Predictor (final model)	OR	95% CI	p-value
Gleason 3+3 (compared to benign)	1.26	0.9-1.9	.24
Gleason 3+4 (compared to benign)	3.1	1.9-4.9	<.001
Gleason ≥4+3 (compared to benign)	8.7	4.5-17.0	<.001
ISUP MCCL (per mm increase)	1.24	1.15-1.33	<.001
$\log_2$ of prostate volume in mL	0.7	0.5-0.9	.02

Note.—A mixed model with random intercepts for individual patients and Gleason grade, Maximum Cancer Core Length (MCCL) as per International Society of Urological Pathology definition and the $\log_2$ of prostate volume (in mL) as fixed predictors had the lowest Akaike Information Criterion and was selected as the final one. The intraclass correlation coefficient was 0.22. Model parameter estimates and corresponding odds ratios (OR) for each predictor are presented with 95% CI (Confidence Interval).

10 E. Doty St., Suite 441, Madison, WI 53703, 630-481-1047, radiology@rsna.org

Table 3: Mixed Models of Non-cancerous Pathology as a Determinant of Zonal MRI Positivity in Men who were TPM-negative (n=52; 1031 Barzell zones)

Model	Predictor	OR	95% CI	p-value
Full	Inflammation	0.8	0.5-1.5	0.49
	PIN	3.2	1.3-8.1	.01
	ASAP	1.9	0.7-5.3	0.21
Final	PIN	3.7	1.5-9.1	.004

Note.—Various combinations of predictors were used. In the full mixed model, the presence of chronic inflammation or Atypical Small Acinar Proliferation (ASAP) did not increase the odds of declaring a zone MRI-visible (see also Supplementary Table 1). A reduced mixed model with random intercepts for individual patients and only Prostatic Intraepithelial Neoplasia (PIN) as a fixed predictor had the lowest Akaike Information Criterion and was thus selected. The intraclass correlation coefficient was 0.49. Model parameter estimates and corresponding odds ratios (OR) for each predictor are presented with 95% CI. TPM-transperineal mapping

Figure Legends

Figure 1a: Patient population and MRI-transperineal mapping (TPM) alignment. The study included 161 PROMIS participants from UCLH (non-pilots) who had multiparametric MRI followed by a combined biopsy procedure and detailed, per-zone recording of Gleason grade and Maximum Cancer Core Length (MCCL) as per International Society of Urological Pathology definition. A consensus multidisciplinary panel, blinded to TPM findings, reviewed MRI images and aligned any lesions with a Likert score ≥ 3 to specific Barzell zones before pathology was revealed; for example, the left PZ lesion shown in the inset was aligned to zones 13,14,17 and 18. **Figure 1b:** In total, the panel determined the MRI positivity of 3179 zones - this was slightly less than the expected 161 x 20 = 3220 due to small prostate size in five men, which did not permit full sampling of all Barzell zones. Of 3179 zones, 2516 were benign, 301 had Gleason 3+3 cancer, 271 Gleason 3+4 and 91 Gleason ≥ 4+3. In total, 595 zones were MRI-positive (18.7%) but the proportion of MRI-visible ones rose with increasing Gleason and with each additional mm in MCCL, motivating a zonal pathology-based model of MRI positivity.

Figure 2a: A moderate age difference between groups (p=0.04; Kruskal Wallis analysis of variance) was primarily driven by the lower median age of the Gleason 3+3 group (21 men). **Figure 2b:** Men with overall Gleason ≥ 4+3 on trans-perineal mapping (TPM) had low prostate volumes compared with other groups (p<0.001, Kruskal-Wallis analysis of variance and adjusted pairwise comparisons) **Figure 2c:** Men with overall Gleason ≥ 4+3 on TPM had high PSA density (PSAD) compared with other groups (p<0.001, Kruskal-Wallis analysis of variance and adjusted pairwise comparisons), and low prostate volumes as shown in the previous figure. In men who were TPM-negative, this relationship was reversed: prostate volume was highest and PSAD lowest. These findings imply the existence of two distinct pathological states in biopsy-naïve men that, although both manifest as elevated PSA requiring a biopsy, differ in terms of the mechanism generating the PSA rise.

Figure 3a: Predicted probabilities of a Barzell zone considered "MRI-visible" using zonal Gleason, Maximum Cancer Core Length (MCCL) and $\log_2$ of prostate volume (in mL) as predictors in a mixed model with random intercepts for patients (3179 zones in 161 men). The probability progressively increases with every increment in Gleason or MCCL, while prostate volume increase has the opposite effect. **Figure 3b:** After selecting the Barzell zones spanning a specific lesion, the expert panel also agreed on a single zone having the "best" alignment. In total, 115 cancerous zones "best" aligned with a lesion (index or secondary), and their pathology against Likert is shown. Higher MCCL was associated higher radiological scores (Likert 4-5), particularly when Gleason pattern 4 was present (p<0.05, Kruskal-Wallis). MCCL less than ~5 mm was mostly associated with Likert 3 lesions (the main arena of true-false positive MRI distinctions), regardless of cancer grade. ISUP-International Society of Urological Pathology

Supplementary Figure Legends

Supplementary Figure 1: The 20-zone modified Barzell zone scheme. All PROMIS participants had mpMRI and underwent 5-mm TPM followed by TRUS biopsy regardless of imaging findings. The Barzell scheme was then used to classify biopsy cores according to the prostatic region from which they were obtained: the prostate is divided in 20 zones in total. Pathology reporting was done per-zone and at the whole prostate level. The Barzell scheme has also been used in other UCLH studies such as Prostate Imaging Compared to Transperineal Ultrasound-guided biopsy for significant prostate cancer Risk Evaluation (PICTURE; Simmons et al. Br J Cancer 2017).

Supplementary Figure 2: UCL definition-based analysis. All cancerous zones were re-classified according to the four UCL definitions of clinical significance, which were considered mutually exclusive in this setting. A mixed model with random intercepts for individual patients and UCL definition category and prostate volume as fixed predictors is presented in the table. The conclusions are similar, in that the presence of csCa significantly raises the odds of a zone deemed MRI-visible, especially in small prostates (A). In addition, csCa in the "most" aligned Barzell zones was clearly associated with high lesion Likert (scores of 4 or 5), whereas clinical insignificance was more observed in Likert 3 zones (B). UCL=University College London, csCa=Clinically Significant Cancer.

Supplementary Tables

Model	Predictors	AIC
Null GLM	Intercept only	3086.948
Null Mixed	Random intercept only	2924.294
Mixed 1	Gleason	2604.279
Mixed 2	Gleason + MCCL	2567.339
Mixed 3 (final)	**Gleason + MCCL + $\log_2$vol**	**2563.581**

Model	Predictors	AIC
Null GLM	Intercept only	753.9745

Null Mixed	Random intercept only	650.1202
Mixed 1	Inflammation + PIN + ASAP	645.1227
Mixed 2	Inflammation + PIN	644.5964
Mixed 3 (final)	**PIN**	**643.1035**

Supplementary Table 1: AIC-based mixed model selection for true (top table) and false (bottom table) MRI positivity. Akaike Information Criterion (AIC) values for all fitted models are presented; mixed models performed better than Generalised Linear Models (GLM) with fixed effects only, while the AIC of the two selected mixed models were the lowest. The addition of interactions led to model non-convergence, so no interaction terms were included. MCCL=Maximum Cancer Core Length, PIN=Prostatic Intraepithelial Neoplasia, ASAP=Atypical Small Acinar Proliferation, log2vol=Binary Logarithm of Prostate Volume in mL.

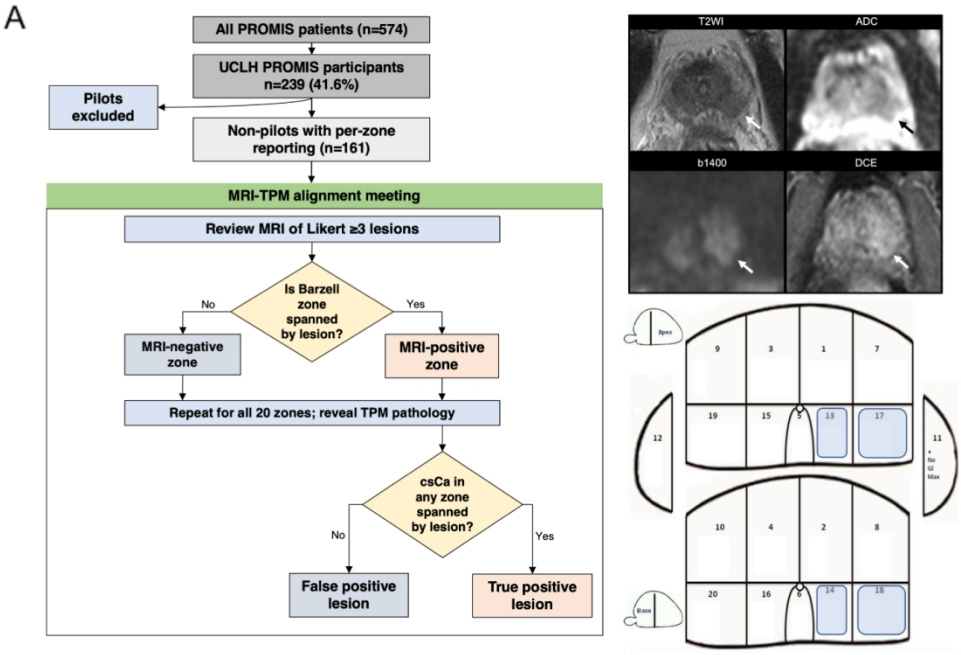

Figure 1a: Patient population and MRI-transperineal mapping (TPM) alignment. The study included 161 PROMIS participants from UCLH (non-pilots) who had multiparametric MRI followed by a combined biopsy procedure and detailed, per-zone recording of Gleason grade and Maximum Cancer Core Length (MCCL) as per International Society of Urological Pathology definition. A consensus multidisciplinary panel, blinded to TPM findings, reviewed MRI images and aligned any lesions with a Likert score ≥ 3 to specific Barzell zones before pathology was revealed; for example, the left PZ lesion shown in the inset was aligned to zones 13,14,17 and 18.

167x117mm (225 x 225 DPI)

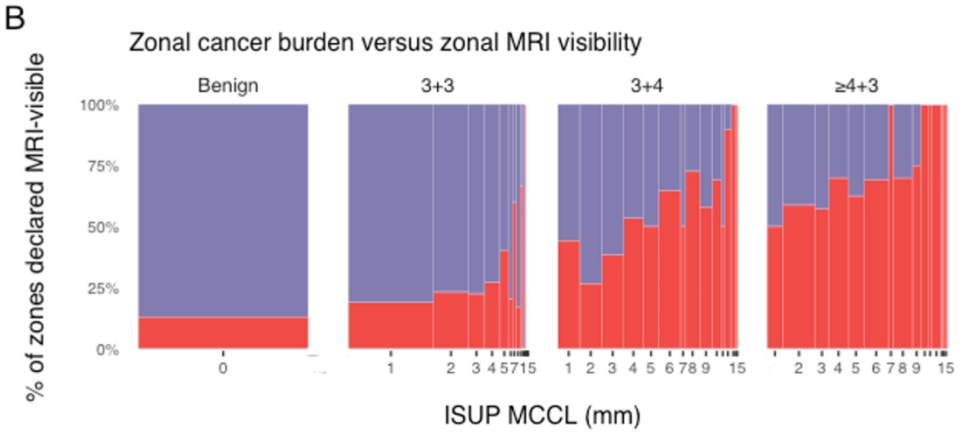

Figure 1b: In total, the panel determined the MRI positivity of 3179 zones - this was slightly less than the expected 161 x 20 = 3220 due to small prostate size in five men, which did not permit full sampling of all Barzell zones. Of 3179 zones, 2516 were benign, 301 had Gleason 3+3 cancer, 271 Gleason 3+4 and 91 Gleason ≥ 4+3. In total, 595 zones were MRI-positive (18.7%) but the proportion of MRI-visible ones rose with increasing Gleason and with each additional mm in MCCL, motivating a zonal pathology-based model of MRI positivity.

164x77mm (225 x 225 DPI)

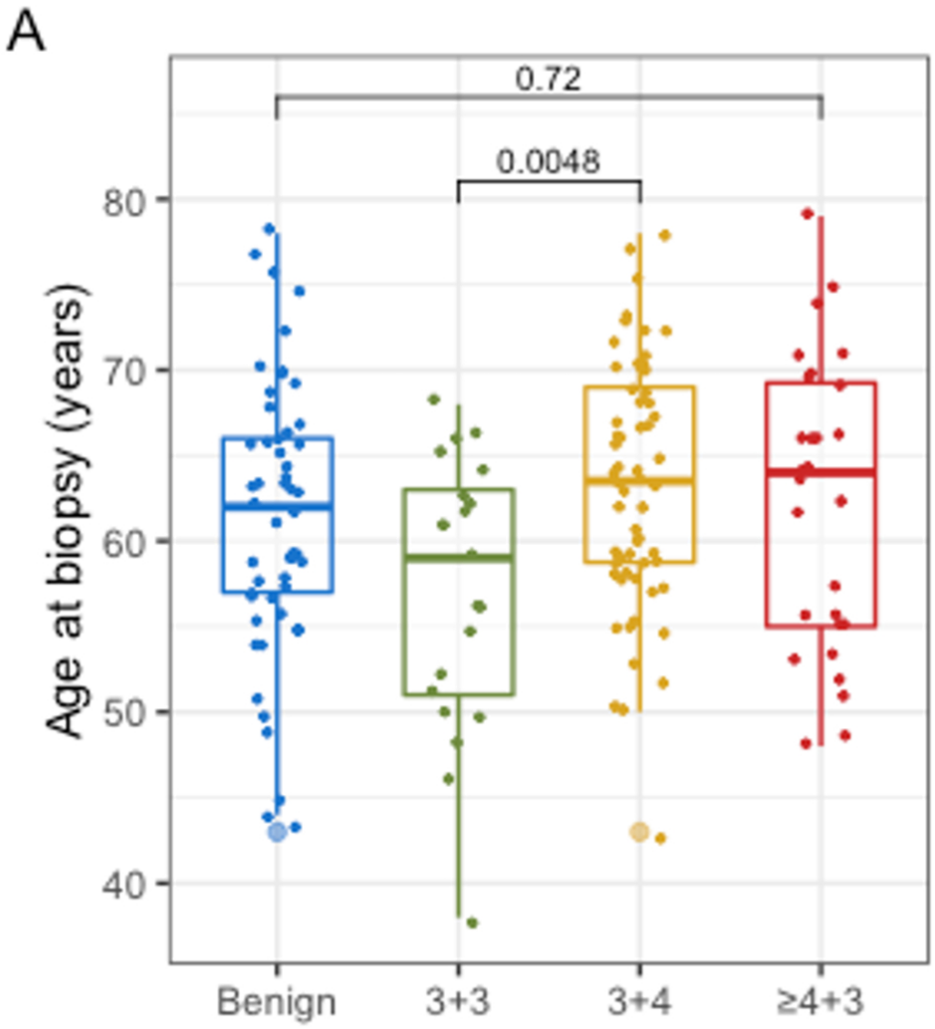

Figure 2a: A moderate age difference between groups (p=0.04; Kruskal Wallis analysis of variance) was primarily driven by the lower median age of the Gleason 3+3 group (21 men).

113x126mm (225 x 225 DPI)

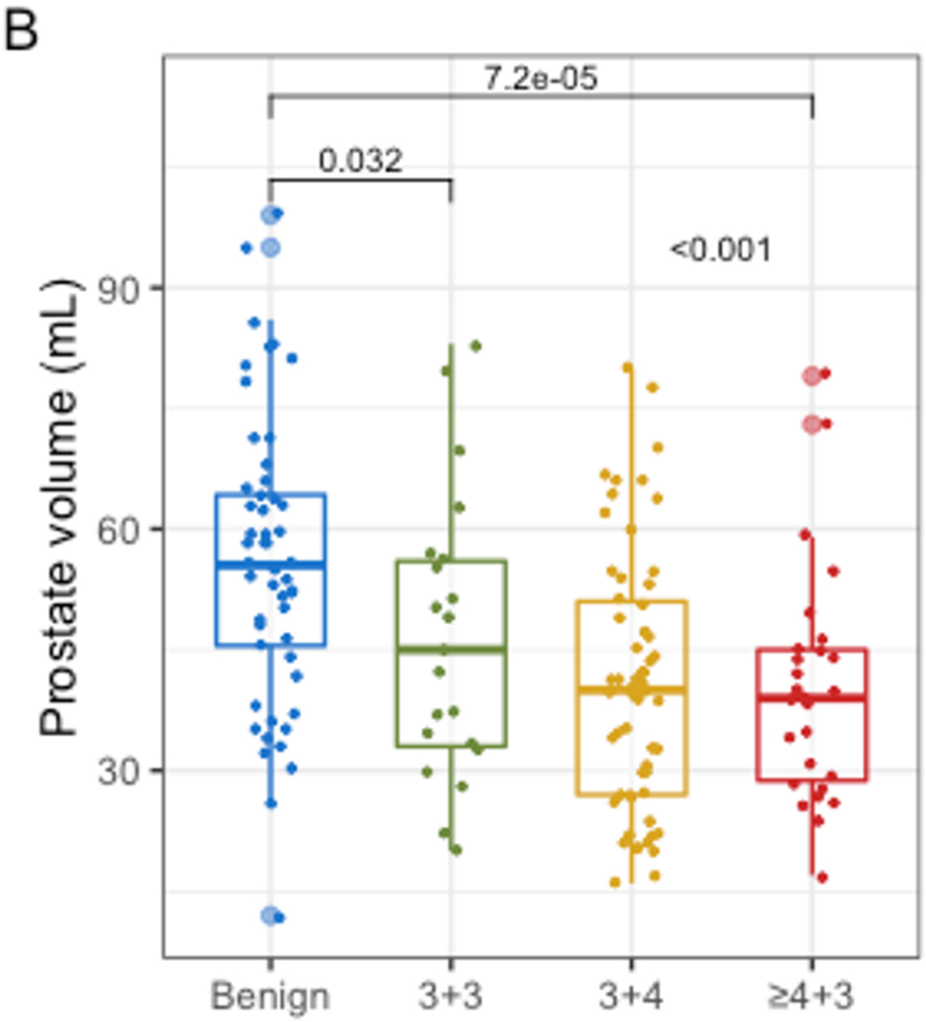

Figure 2b: Men with overall Gleason ≥ 4+3 on trans-perineal mapping (TPM) had low prostate volumes compared with other groups (p<0.001, Kruskal-Wallis analysis of variance and adjusted pairwise comparisons).

113x127mm (225 x 225 DPI)

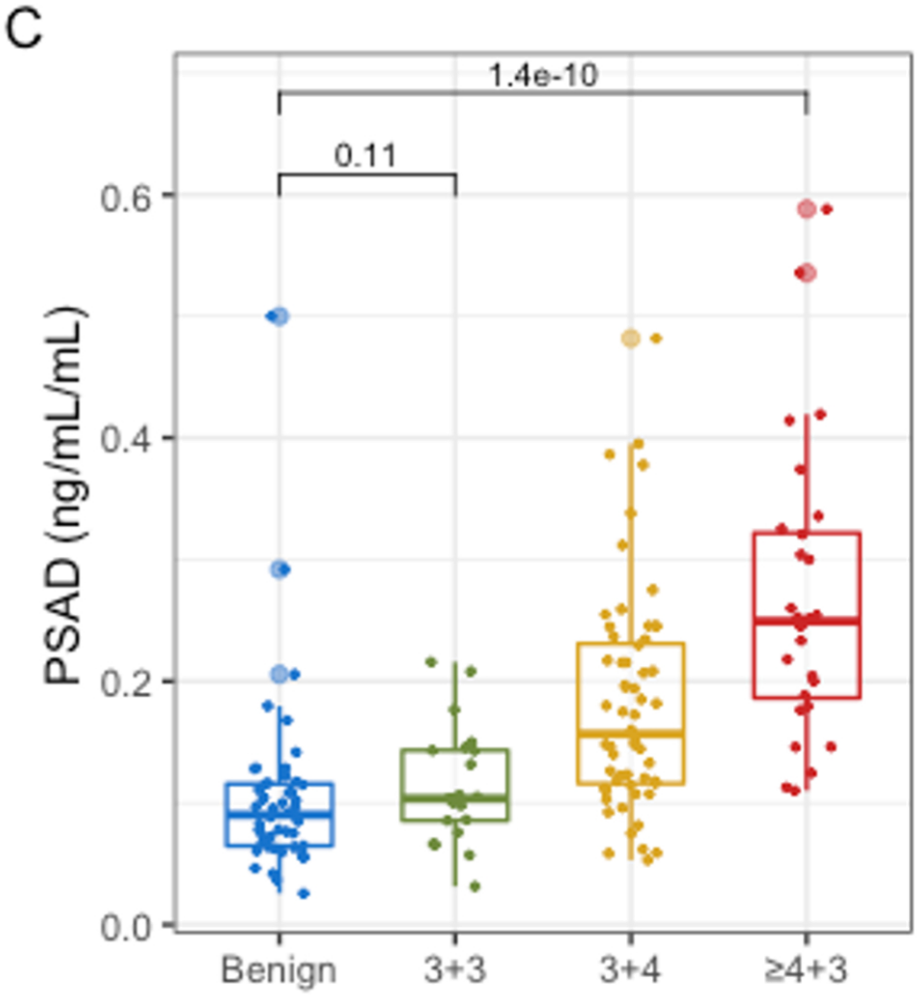

Figure 2c: Men with overall Gleason ≥ 4+3 on TPM had high PSA density (PSAD) compared with other groups ($p<0.001$, Kruskal-Wallis analysis of variance and adjusted pairwise comparisons), and low prostate volumes as shown in the previous figure. In men who were TPM-negative, this relationship was reversed: prostate volume was highest and PSAD lowest. These findings imply the existence of two distinct pathological states in biopsy-naïve men that, although both manifest as raised PSA requiring a biopsy, differ in terms of the mechanism generating the PSA rise.

116x126mm (225 x 225 DPI)

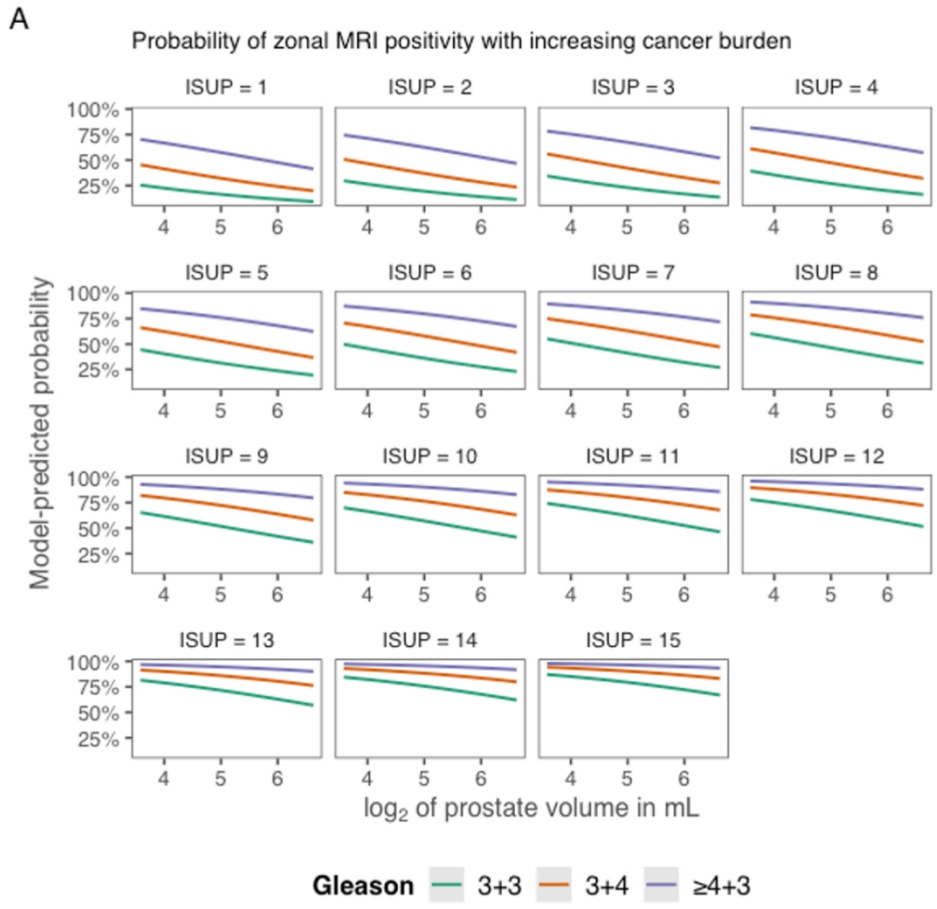

Figure 3a: Predicted probabilities of a Barzell zone considered "MRI-visible" using zonal Gleason, Maximum Cancer Core Length (MCCL) and log2 of prostate volume in mL as predictors in a mixed model with random intercepts for patients (3179 zones in 161 men). The probability progressively increases with every increment in Gleason or MCCL, while prostate volume increase has the opposite effect.

137x131mm (225 x 225 DPI)

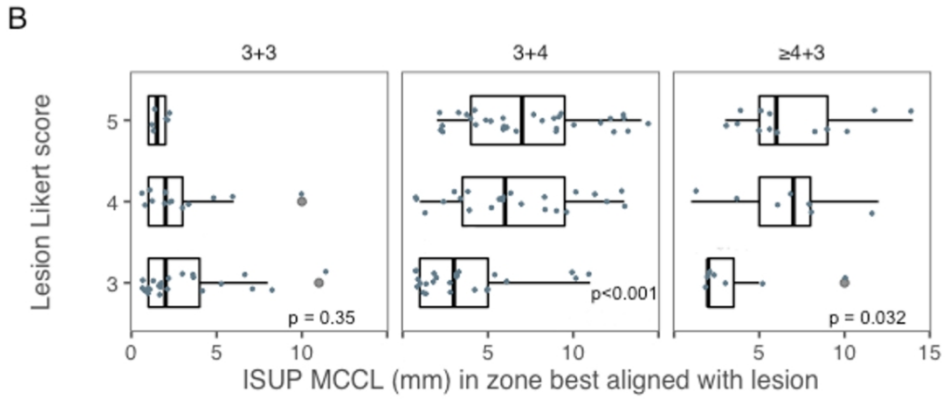

Figure 3b: After selecting the Barzell zones spanning a specific lesion, the expert panel also agreed on a single zone having the "best" alignment. In total, 115 cancerous zones "best" aligned with a lesion (index or secondary), and their pathology against Likert is shown. Higher MCCL was associated higher radiological scores (Likert 4-5), particularly when Gleason pattern 4 was present ($p<0.05$, Kruskal-Wallis). MCCL less than ~5 mm was mostly associated with Likert 3 lesions (the main arena of true-false positive MRI distinctions), regardless of cancer grade. ISUP- International Society of Urological Pathology

137x60mm (225 x 225 DPI)

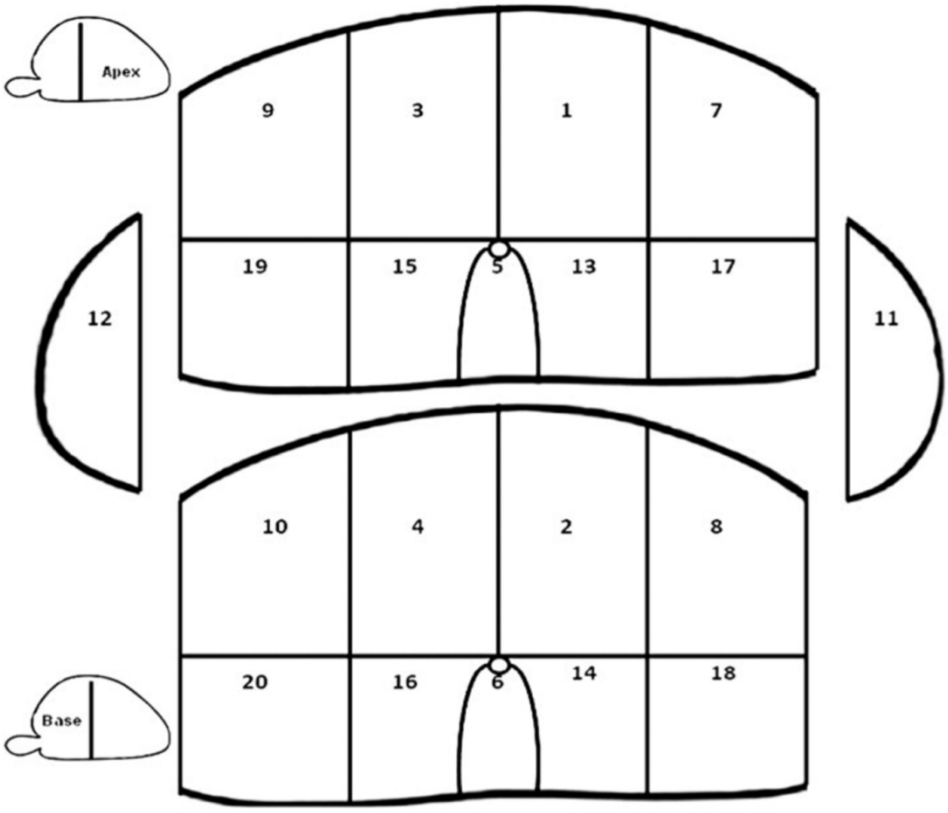

Modified Barzell Zones

1 Left Parasagital Anterior Apex
2 Left Parasagital Anterior Base
3 Right Parasagital Anterior Apex
4 Right Parasagital Anterior Base
5 Midline Apex
6 Midline Base
7 Left Medial Anterior Apex
8 Left Medial Anterior Base
9 Right Medial Anterior Apex
10 Right Medial Anterior Base
11 Left Lateral
12 Right Lateral
13 Left Parasagital Posterior Apex
14 Left Parasagital Posterior Base
15 Right Parasagital Posterior Apex
16 Right Parasagital Posterior Base
17 Left Medial Posterior Apex
18 Left Medial Posterior Base
19 Right Medial Posterior Apex
20 Right Medial Posterior Base

Supplementary Figure 1: The 20-zone modified Barzell zone scheme. All PROMIS participants had mpMRI and underwent 5-mm TPM followed by TRUS biopsy regardless of imaging findings. The Barzell scheme was then used to classify biopsy cores according to the prostatic region from which they were obtained: the prostate is divided in 20 zones in total. Pathology reporting was done per-zone and at the whole prostate level. The Barzell scheme has also been used in other UCLH studies such as Prostate Imaging Compared to Transperineal Ultrasound-guided biopsy for significant prostate cancer Risk Evaluation (PICTURE; Simmons et al. Br J Cancer 2017).

169x188mm (220 x 220 DPI)

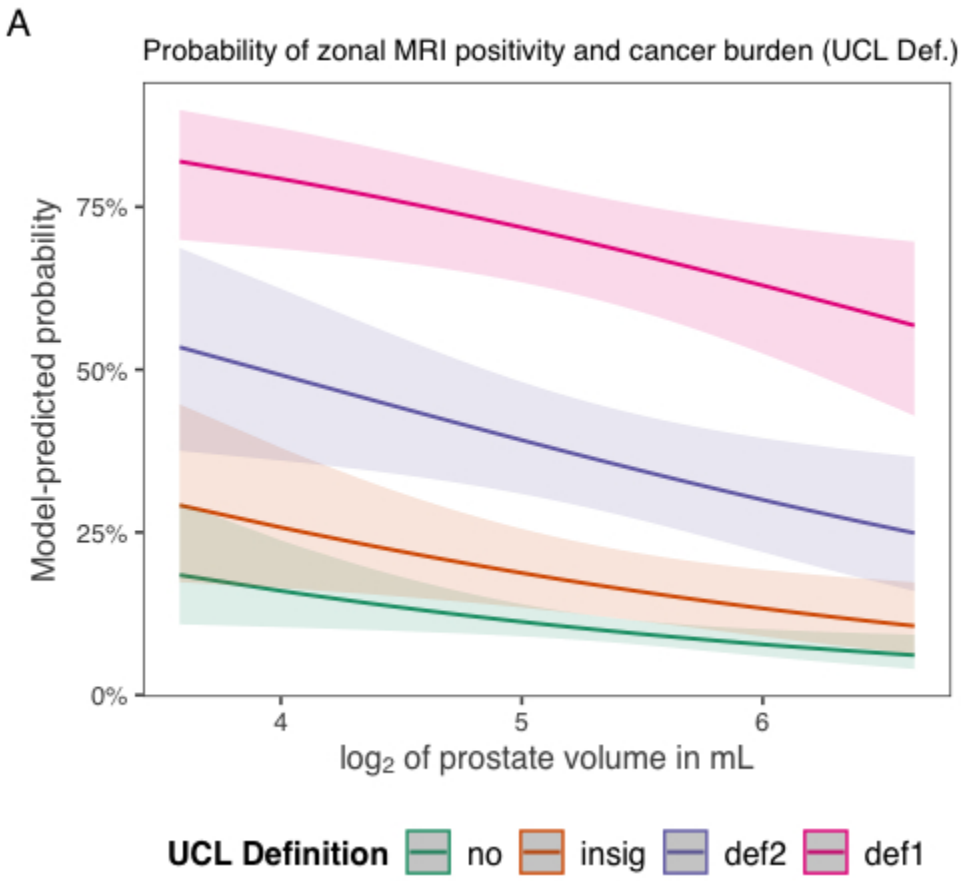

Supplementary Figure 2A: UCL definition-based analysis. All cancerous zones were re-classified according to the four UCL definitions of clinical significance, which were considered mutually exclusive in this setting. A mixed model with random intercepts for individual patients and UCL definition category and prostate volume as fixed predictors is presented in the table. The conclusions are similar, in that the presence of csCa significantly raises the odds of a zone deemed MRI-visible, especially in small prostates (A). In addition, csCa in the "most" aligned Barzell zones was clearly associated with high lesion Likert (scores of 4 or 5), whereas clinical insignificance was more observed in Likert 3 zones (B). UCL=University College London, csCa=Clinically Significant Cancer.

175x167mm (72 x 72 DPI)

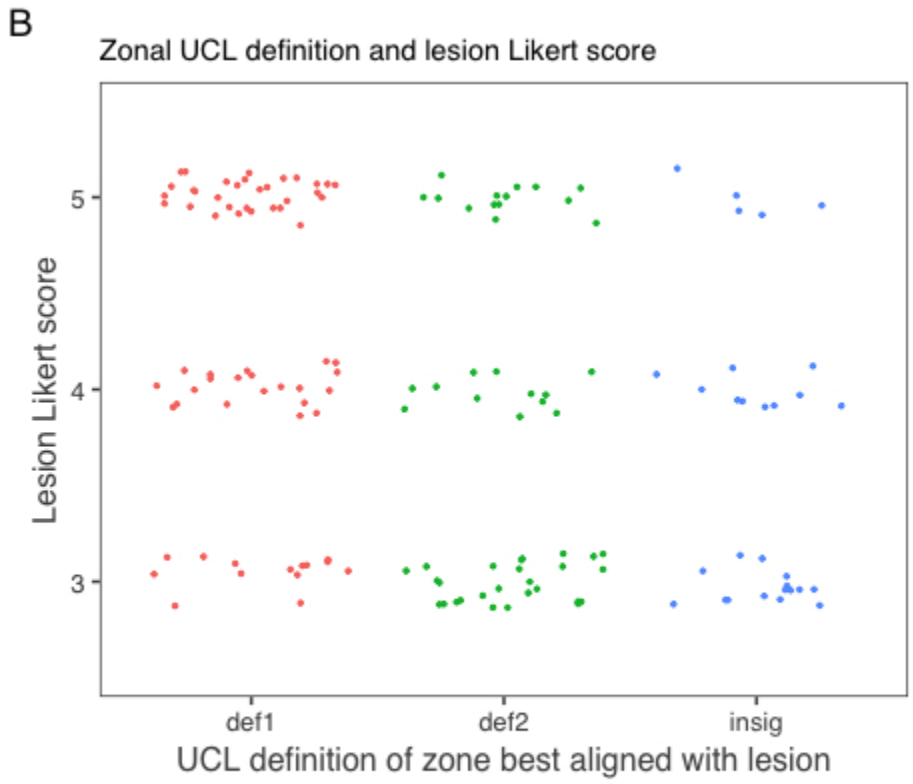

Supplementary Figure 2B: UCL definition-based analysis. All cancerous zones were re-classified according to the four UCL definitions of clinical significance, which were considered mutually exclusive in this setting. A mixed model with random intercepts for individual patients and UCL definition category and prostate volume as fixed predictors is presented in the table. The conclusions are similar, in that the presence of csCa significantly raises the odds of a zone deemed MRI-visible, especially in small prostates (A). In addition, csCa in the "most" aligned Barzell zones was clearly associated with high lesion Likert (scores of 4 or 5), whereas clinical insignificance was more observed in Likert 3 zones (B). UCL=University College London, csCa=Clinically Significant Cancer.

166x167mm (72 x 72 DPI)

Regional histopathology and prostate MRI positivity: a secondary analysis of the PROMIS trial

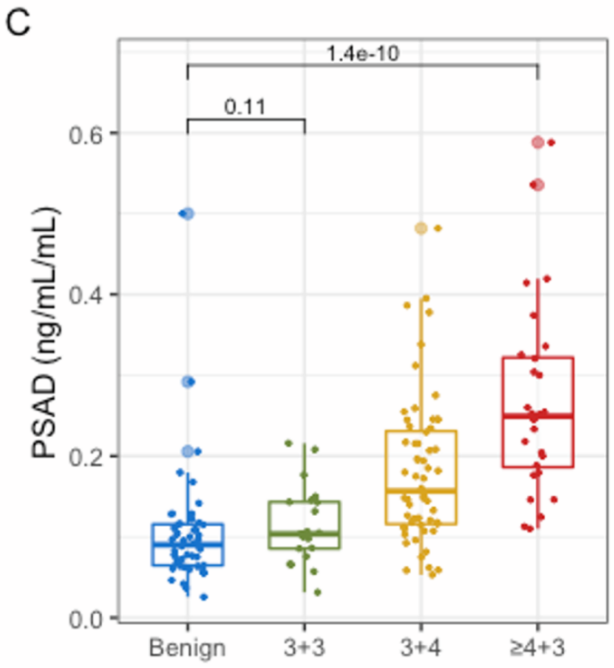

- In 161 men from the PROMIS trial, prostate zones that contained Gleason 3+4 cancer were three times more likely to be MRI-positive than benign zones (OR: 3.1 p<0.001), and almost nine times if they contained Gleason ≥4+3 (OR: 8.7, p<0.001).
- Increasing maximum cancer core length raised the odds of a cancerous zone being MRI-positive (OR: 1.24 per mm increase, p<0.001).
- In cancer-free prostates, zones containing prostatic intraepithelial neoplasia were more likely to be MRI-positive (OR: 3.7, p=0.004).

Stavrinides V et al. Published Online: DATE, 2022
https://doi.org/10.1148/radiol.220762

Radiology